[illegible]

NASA TN D-1075

393639

TECHNICAL NOTE

D-1075

SOME EFFECTS OF LEADING-EDGE SWEEP ON BOUNDARY-LAYER TRANSITION AT SUPERSONIC SPEEDS

By Gary T. Chapman

Ames Research Center
Moffett Field, Calif.

NATIONAL AERONAUTICS AND SPACE ADMINISTRATION
WASHINGTON September 1961

NASA TN D-1075

NATIONAL AERONAUTICS AND SPACE ADMINISTRATION

TECHNICAL NOTE D-1075

SOME EFFECTS OF LEADING-EDGE SWEEP ON BOUNDARY-LAYER TRANSITION AT SUPERSONIC SPEEDS

By Gary T. Chapman

SUMMARY

The effects of crossflow and shock strength on transition of the laminar boundary layer behind a swept leading edge have been investigated analytically and with the aid of available experimental data.

An approximate method of determining the crossflow Reynolds number on a leading edge of circular cross section at supersonic speeds is presented. The applicability of the critical crossflow criterion described by Owen and Randall for transition on swept wings in subsonic flow was examined for the case of supersonic flow over swept circular cylinders. A wide range of applicability of the subsonic critical values is indicated. The corresponding magnitude of crossflow velocity necessary to cause instability on the surface of a swept wing at supersonic speeds was also calculated and found to be small.

The effects of shock strength on transition caused by Tollmien-Schlichting type of instability are discussed briefly. Changes in local Reynolds number, due to shock strength, were found analytically to have considerably more effect on transition caused by Tollmien-Schlichting instability than on transition caused by crossflow instability. Changes in the mechanism controlling transition from Tollmien-Schlichting instability to crossflow instability were found to be possible as a wing is swept back and to result in large reductions in the length of laminar flow.

INTRODUCTION

The need for swept wings on hypersonic vehicles to reduce the leading-edge heat transfer and leading-edge drag has been well recognized. The sweep of the wing, however, has a large adverse effect on transition of the laminar boundary layer and causes a relative increase in turbulent wetted area with accompanying higher heating rate and higher drag. Various reasons for this adverse effect of sweep on transition of the laminar boundary layer have been postulated. Furthermore, several phenomena may operate simultaneously to affect transition in different ways, thereby making the problem exceedingly complex.

There are at least two basic effects on the local flow which result from sweeping a wing: (1) crossflow resulting from spanwise pressure gradients (The effect of crossflow on transition was first recognized and studied by Owen and Randall (ref. 1) at subsonic speeds.); (2) leading-edge shock-wave effects due to changes in shock strength with sweep (The effect of shock strength on transition, first studied by Moeckel (ref. 2) with respect to blunting of wedges and cones, is to reduce the local Reynolds number thereby increasing the length of laminar flow.).

The purpose of the present report is to discuss the above effects and their relation to the over-all problem of boundary-layer transition on swept wings. This discussion includes a brief summary statement of some earlier results, and also includes development and presentation of new results. The new results are obtained from analysis and from study of available experimental data. Principal new results are in the areas of a crossflow instability criterion for supersonic speeds, the influence of bow-shock-wave strength on crossflow instability, and the necessary thickness of an entropy layer to be effective in postponing transition.

SYMBOLS

D	diameter of leading edge
M	Mach number
p	pressure
R	Reynolds number based on x, $\frac{\rho U x}{\mu}$
R_T	transition Reynolds number, $\frac{\rho_\infty U_\infty x_l}{\mu_\infty}$
T	temperature
U	resultant velocity
w	velocity parallel to surface and normal to boundary-layer-edge streamline measured in a plane parallel to the local tangent plane
x	distance from leading edge, parallel to center line
y	distance normal to local tangent plane
β	crossflow velocity parameter, $\frac{w}{U_e}$
γ	ratio of specific heat at constant pressure to that at constant volume

δ	boundary-layer thickness
θ	position angle on circular cylinder, 0 at stagnation line
Λ	sweep angle of wing leading edge
μ	coefficient of viscosity
ρ	air density
τ	thickness of high entropy layer
χ	crossflow Reynolds number (See eq. (1).)
ω	exponent in viscosity relationship, $\frac{\mu}{\mu_\infty} = \left(\frac{T}{T_\infty}\right)^\omega$

Subscripts

e	boundary-layer-edge conditions
l	laminar
max	maximum value
s	wing leading-edge stagnation line
t	stagnation condition
w	wall conditions
o	free-stream stagnation conditions
∞	free-stream static conditions
M_N	Mach number normal to leading edge at a given sweep angle

ANALYSIS AND DISCUSSION

Crossflow Effects

Wings with sweptback leading edges and finite thickness will, in general, develop spanwise pressure gradients. These gradients give rise to crossflow, or secondary flow, as it is sometimes referred to, which can be an important consideration in the transition of the laminar boundary layer on swept wings. Shown in sketch (a) is a typical crossflow velocity profile. This is the velocity profile which occurs normal to the boundary-layer edge streamline. It can be shown that this profile has both a maximum and an inflection point.

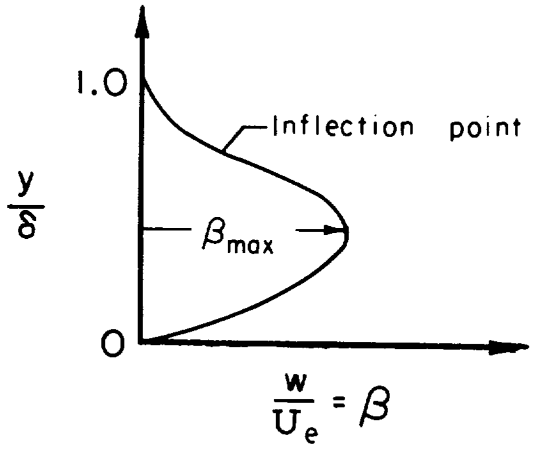

Sketch (a)

Crossflow instability.- In their studies of transition on swept wings at subsonic speeds, Owen and Randall (ref. 1) found that crossflow had an adverse effect on laminar boundary-layer stability. They showed evidence of a system of uniformly spaced vortices in the boundary layer with axes parallel to the stream direction. The vortices are believed to result from the inflection point in the crossflow velocity profile. Later, Gregory, Stuart, and Walker (ref. 3) showed theoretically that the crossflow velocity profile is unstable to small disturbances.

Owen and Randall further found that they could correlate the abrupt formation of these streamwise vortices and also the development of complete turbulence (i.e., transition) with a crossflow Reynolds number, χ, defined by:

$$\chi \equiv \frac{\rho_e w_{max} \delta}{\mu_e} \tag{1}$$

where w_{max} is the maximum crossflow velocity. They found the critical values of crossflow Reynolds number for vortex formation and for transition to be 125 and 175, respectively. These values were for regions very near the leading edge of swept wings at subsonic speeds. More recent work by Boltz, Kenyon, and Allen (ref. 4), also at subsonic speeds but including regions farther downstream of the leading edge, gives values of 135 to 190 for vortex formation and 190 to 260 for transition.[1] Some work by Scott-Wilson and Capp at Mach number 1.61 (ref. 5) indicates that these values may be somewhat smaller in supersonic flow. However, because of the complexity of calculating the compressible laminar boundary layer over three-dimensional surfaces, no numerical values of critical crossflow Reynolds number have been established for supersonic flow past swept wings. Because of this complexity, the more limited case of supersonic flow over a swept circular cylinder will be considered.

---

[1] In view of the approximations made for the calculation of the crossflow Reynolds number and the difference in test conditions (e.g., stream turbulence level), the agreement between the results of references 1 and 4 is considered to be good.

Crossflow on a circular leading edge.- In the present paper, a method is developed to calculate the crossflow Reynolds number on a circular leading edge by means of Reshotko and Beckwith's (ref. 6) stagnation-line solution for a swept circular cylinder. It is assumed that the form of dimensionless velocity profile is unaltered around the semicircular leading edge, and that the boundary-layer thickness over the leading edge is constant and equal to the stagnation-line value. The velocity profile assumption has only limited range of validity in the exact sense (ref. 6), but for engineering accuracy the results indicate it may be fairly good over the entire leading edge. The boundary-layer thickness assumption is also limited in the exact sense; however, calculations performed on a hemisphere (ref. 7) show increases of less than 30 percent of the stagnation-point boundary-layer thickness over most of the hemisphere. The growth of the boundary layer on a circular cylinder would probably be somewhat larger because of the divergence exhibited by the flow field around a hemisphere. However, it was thought that for a first approximation the simpler approach would be adequate. These assumptions, along with perfect gas relations and a power law dependence of viscosity on temperature may be used to write the crossflow Reynolds number:

$$\chi = \left(R_\infty \frac{D}{x}\right)^{1/2} \beta_{max} HB \frac{(T_0/T_\infty)^{\frac{\omega+1}{2}} (T_w/T_0)^{\frac{\omega-1}{2}}}{[G(p_s/p_\infty)]^{1/2}} \tag{2}$$

where B and G are defined in appendix A; β_{max}, the maximum value of the crossflow velocity ratio, is found by the method given in appendix B; and H, the ratio of local to free-stream unit Reynolds number, is given by equation (C4) of appendix C. The details of the development of equation (2) may be found in appendixes A, B, and C.

Equation (2) is similar in form to an equation derived in reference 8 for a swept circular cylinder in incompressible flow. Equation (2), however, is for supersonic flow with heat transfer and therefore includes effects of Mach number and temperature ratio, not considered in reference 8.

Presented in figure 1 is an example of the crossflow properties calculated by the method described in appendixes A, B, and C; a leading-edge sweep on 60°, free-stream Mach number of 7.0, and a ratio of wall temperature to total temperature of 0.60 were used for the example. Figure 1(a) shows maximum values of the crossflow velocity ratio, β_{max}, as a function of the body coordinate, θ. Figure 1(b) shows the value of $\chi/[R_\infty(D/x)]^{1/2}$ as a function of θ, also. A maximum value of $\chi/[R_\infty(D/x)]^{1/2}$ occurs at $\theta = 60^\circ$. This would indicate that transition could move rapidly to this point rather than approach this point continuously from the downstream side.

With the aid of equation (2) and available experimental data (refs. 8 to 11) it was possible to evaluate critical values of crossflow Reynolds number for swept circular cylinders in supersonic flow. Maximum values of crossflow Reynolds number were computed for the test conditions of references 8 through 11 and compared with the state of the boundary layer (i.e., laminar or turbulent) on the leading edge.

The actual state of the boundary layer on the leading edge was not given directly in references 8 to 11 but could be inferred from a comparison of the heat-transfer data with heat-transfer values predicted from well-established laminar heat-transfer theories. The boundary layer was considered to be turbulent if the heat transfer was appreciably higher than laminar theory would predict. Data about which there was doubt as to the state of the boundary layer were designated transitional. There was some question as to the interpretation of a result from reference 10 at a Mach number of 6.9 and a sweep angle of 75°. Feller (ref. 10) indicates that three-dimensional effects due to the apex at large sweep angles accounted for the higher heat transfer. These data were analyzed also by Goodwin and Creager (ref. 11) who showed that not only was the datum at 75° of sweep considerably above the laminar theoretical predictions but that the datum for 60° of sweep also deviated from the laminar theory. It seems unlikely that the datum for 60° of sweep is influenced by the apex. This becomes more evident on comparing the region of influence of the apex (i.e., the Mach cone from the apex) and the apex angle, 8.25° and 30°, respectively. It is therefore felt that the high heat transfer at 75° of sweep is not due to the apex but is a result of increased extent of turbulent flow which has already begun to show itself at 60° of sweep. On this basis, the data of reference 10 at 60° and 75° of sweep were interpreted as transitional and turbulent, respectively.

The results are presented in table I and in figure 2, where the maximum calculated value of crossflow Reynolds number occurring on the leading edge, for each test condition, is plotted as a function of free-stream Mach number. The solid symbols represent cases of turbulent boundary-layer flow; the open symbols, laminar; and the half-filled symbols, transitional. Included for comparison in figure 2 are the critical values determined by Owen and Randall (ref. 1) and by Boltz, Kenyon, and Allen (ref. 4). These values are represented by lines and cross-hatched areas, respectively. The comparison with the higher Mach number data appears to indicate that these critical values are constant over a considerable Mach number range.

Values of crossflow Reynolds number of less than 100 appear to give reasonable assurance of complete laminar flow on the leading edge.

Crossflow downstream of the leading edge.- If the boundary layer on the leading edge is not destabilized sufficiently for transition to be caused by crossflow, transition may still be caused by crossflow farther back on the wing, provided, of course, that the streamwise velocity profile does not become unstable first. Because of the complexity of the exact compressible laminar-boundary-layer equations for a general surface, no simple formula for determining the crossflow in this area seems possible. However, a relationship between the crossflow Reynolds number, χ, the local Reynolds number, R_e, and the crossflow velocity ratio, β_{max}, can be established from which, with the aid of experimental results, it is possible to estimate the amount of crossflow necessary to cause transition.

If we assume that the boundary-layer thickness for a swept wing can be given approximately by the flat-plate two-dimensional values, that is,

$$\delta = Kx/\sqrt{R_e} \tag{3}$$

where $K = K(M_e, T_w/T_o)$ as defined in reference 12, the crossflow Reynolds number may be written

$$\chi = K\sqrt{R_e}\,\beta_{max} \tag{4}$$

In figure 3 values of the crossflow velocity ratio, β_{max}, calculated using equation (4), are plotted as a function of local Reynolds number for a critical crossflow Reynolds number of 175 and values of K of 8 and 10. The curves in this figure, which represent transition Reynolds number as a function of the crossflow parameter, show that even relatively small values of the crossflow parameter result in small values of transition Reynolds number (e.g., if $K = 10$ and $\beta_{max} = 0.01$, the $R_T = 3$ million). At this point we still cannot use equation (4) to calculate transition Reynolds number because of the complexity of calculating β_{max}. However, if experimental transition Reynolds numbers are used, where transition is thought to be controlled by crossflow, the crossflow velocity that caused transition in these experiments may be estimated.

References 13 and 14 give values of transition Reynolds numbers for tests where transition was considered to be controlled by crossflow. In reference 13 the value of transition Reynolds number for a wing with 75° of sweep, a biconvex airfoil section at a Mach number of 5.35, and a wall-to-total-temperature ratio of 0.27 was given as 4.36 million. Similarly, in reference 14, for a wing with 60° of sweep, an NACA 65A004 airfoil section at a Mach number of 4.04, and a wall-to-total-temperature ratio of about 1, the transition Reynolds number was given as 0.95 million. With these data and equation (4) the values of the crossflow velocity that caused transition are estimated to be 1.0 and 1.8 percent of the local velocity for the tests of references 13 and 14, respectively.

Considering the small amount of crossflow needed to cause transition, it is felt that the transition Reynolds number could be evaluated for wings if crossflow were assumed to be small. This should make it easier to solve the compressible boundary-layer equations for the crossflow velocity ratio, β_{max}. Furthermore, it may be concluded that on wings with large spanwise pressure gradients, transition is more likely to be caused by instability of the crossflow than by instability of the streamwise velocity profile (i.e., Tollmien-Schlichting instability) because of the extremely small amount of crossflow needed to cause transition at small values of the local Reynolds number.

Shock Strength Effects

Another effect of sweep on transition is associated with the reduction in strength of the leading-edge shock wave. This effect always occurs with blunt wings with supersonic leading edges and must be considered with both crossflow instability and Tollmien-Schlichting instability. The effects of shock strength on flow properties are well known, as are the effects of shock strength on transition caused by Tollmien-Schlichting instability. However, a brief discussion of each will be presented here to clarify further the effects of shock strength on crossflow instability, as well as to allow for a discussion of a hypothetical example involving both types of instability.

The effect of shock strength is to increase entropy and thus to alter the flow properties downstream of the shock wave. The greatest change in flow properties occurs behind the strongest portion of the shock wave. This change results in a relatively thin layer over the surface of a wing, downstream of a blunt leading edge, within which the flow properties are significantly different from those in the outer flow field. Within this so-called high-entropy layer, the local unit Reynolds number is lower than it would have been in the absence of the high-entropy layer. Hence, in general, transition is delayed and more laminar flow results. This phenomenon was first studied theoretically by Moeckel (ref. 2) with regard to the blunting of wedges and cones and was observed experimentally by Brinnich and others (refs. 14 to 16).

The effectiveness of the high-entropy layer in delaying transition depends upon its thickness relative to the boundary-layer thickness. Based on the experimental results of references 14 to 16, figure 4 shows that when the high-entropy layer thickness, τ (referred to as low Mach number layer in ref. 2) computed by the method of reference 2, exceeds 30 to 40 percent of the boundary-layer thickness, computed by the method of reference 12, no further delay of transition occurs with further thickening of the high-entropy layer. This method of presentation is preferred to the method of displacing the outer edge of the high-entropy layer by the displacement thickness of the boundary layer as it is felt that the latter loses physical significance for high-entropy layers thinner than the boundary layer. Figure 4 also indicates that a straight line approximation between τ/δ of 0 and 35 percent could be used for rough estimates of intermediate values of transition Reynolds number.

It is evident that if an unswept wing, which has been blunted sufficiently to obtain full benefit of the high-entropy layer, is swept back, the shock strength decreases, resulting in an increase in the local unit Reynolds number and a change in the shear-layer thickness. How these changes effect transition depends on the type of instability controlling transition. However, for the purpose of further discussions we will assume that the high-entropy layer is fully effective at all sweep angles.

The effects of changes in shock strength, due to sweep, on transition controlled by Tollmien-Schlichting instability were discussed briefly by Beckwith and Gallagher (ref. 8). Their results were for a specific test condition, with no explicit details as to how the calculations were made. However, it is a simple matter to derive a relationship for the length of laminar flow for swept wings, assuming that the transition Reynolds number based on local properties is constant. This is done in appendix C, where it is shown that the ratio of length of laminar flow, x_l, for arbitrary sweep to that at zero sweep, $(x_l)_{\Lambda=0}$, for a slightly blunted flat plat at a constant free-stream unit Reynolds number is given by

$$\frac{(x_l)_\Lambda}{(x_l)_{\Lambda=0}} = \frac{(M_e)_{\Lambda=0}}{(M_e)_\Lambda}\left[\frac{1+\frac{\gamma-1}{2}(M_e)^2_{\Lambda=0}}{1+\frac{\gamma-1}{2}(M_e)^2_\Lambda}\right]^{\frac{2\omega+1}{2}} \tag{5}$$

where the values of local Mach number, M_e, for both the swept and the unswept case are found using the relations given by equations (C11).

In figure 5 are plotted solutions of equation (5) as a function of sweep angle for various free-stream Mach numbers ($\gamma = 1.4$, $\omega = 0.8$). It is seen that the relative length of laminar flow decreases very rapidly with increasing sweep. It also shows that this relative decrease is more rapid for higher Mach numbers. It should be noted, however, that the normalizing length of laminar flow, $(x_l)_{\Lambda=0}$, in equation (5) is a function of the free-stream Mach number; therefore figure 5 should not be used to determine the effect of Mach number at a fixed sweep angle on the length of laminar flow, x_l. The same approach as in appendix C can be used to give the ratio of length of laminar flow at an arbitrary Mach number, x_l, to length of laminar flow when the normal Mach number is unity, $(x_l)_{M_N=1}$, for a swept flat plate,

$$\frac{x_l}{(x_l)_{M_N=1}} = \frac{M_\infty}{M_e}\left[\frac{1 + \frac{\gamma-1}{2} M_\infty^2}{1 + \frac{\gamma-1}{2} M_e^2}\right]^{\frac{2\omega+1}{2}} \tag{6}$$

where M_e for arbitrary free-stream Mach number greater than $1/\cos \Lambda$ is found from the relations given by equations (C11). In the derivation of equation (6) it is assumed that the only effect of Mach number is to change the leading-edge shock-wave strength. Results of equation (6) are presented in figure 6 as a function of free-stream Mach number for fixed values of sweep angle. A strong increase in the length of laminar flow, x_l, with increasing Mach number is evident. The curve for zero sweep is similar to one given by Moeckel (ref. 2).

The effect of shock strength on the crossflow Reynolds number on the leading edge, and thereby on transition caused by crossflow instability, is given implicitly in equation (2). For the case of crossflow instability downstream of the leading edge, the effect of shock strength on the length of laminar flow is not as simple as for the case of transition caused by Tollmien-Schlichting instability. This is due to the fact that the crossflow velocity ratio, β_{max}, varies with distance from the leading edge as well as with many other factors. Since no similarity-type solutions exist at present for calculating β_{max}, each case has to be treated separately. However, it was shown in equation (4) that the crossflow Reynolds number, downstream of the leading edge, was proportional to the local Reynolds number to the 1/2 power. Hence, it would appear that influence of shock strength on transition caused by crossflow will not be as strong as on transition controlled by Tollmien-Schlichting instability.

Up to this point the effects of shock strength on transition have been treated separately for crossflow instability and Tollmien-Schlichting instability. However, in the course of a test or flight of a vehicle, both types of instability may exist. In addition, the type controlling transition may change during the course of a flight. As an example of this, consider a variable sweep wing operating at a constant Mach number. At zero sweep, transition is generally controlled by Tollmien-Schlichting instability. As the wing is swept back, transition will move forward as a result of the reduced shock strength (see sketch (b)). When at some point upstream of the transition front, the critical crossflow Reynolds number is exceeded, transition moves forward rapidly. As the wing is swept further, transition continues to move forward, because of the reduced shock strength and increased crossflow, until at some higher sweep angle, provided the flight Reynolds number based on the leading-edge diameter is large enough, the crossflow becomes critical at the leading edge. Here transition again moves rapidly forward.

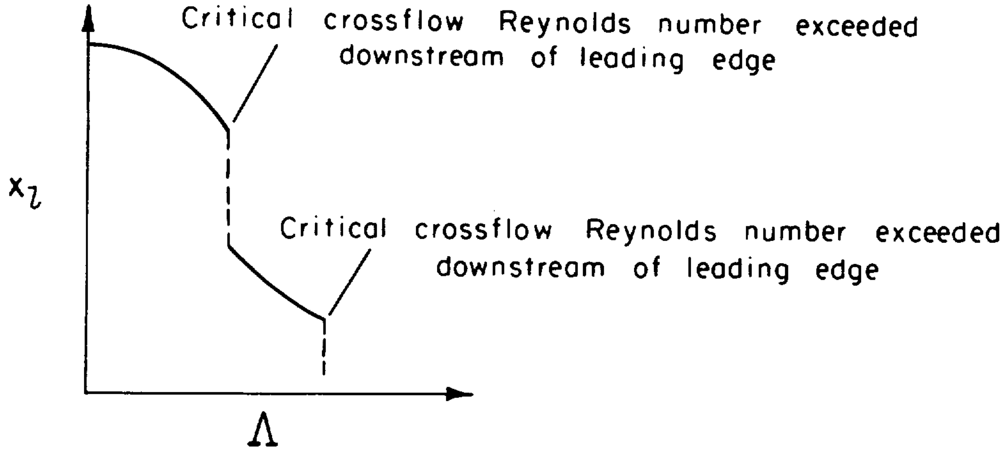

Sketch (b)

A
4
6
1

This last step implies that there can be two peaks in the curve of crossflow Reynolds number as a function of distance downstream of the leading edge (see sketch (c)). Sketch (c) shows a possible streamwise distribution of crossflow Reynolds number over a wing. Whether two peaks should exist in this variation is not known at this time; however, it appears possible, if a sudden drop in χ around the leading edge exists, as exhibited in figure 1(b), and only a very small amount of crossflow velocity is required to obtain a critical value of χ in regions where the boundary layer is thick (i.e., regions far downstream of the leading edge). The trend with sweep angle given in sketch (c) may be qualitatively correct for moderate values of sweep; however, the trend will differ for large values of sweep because at 90° there is no crossflow.

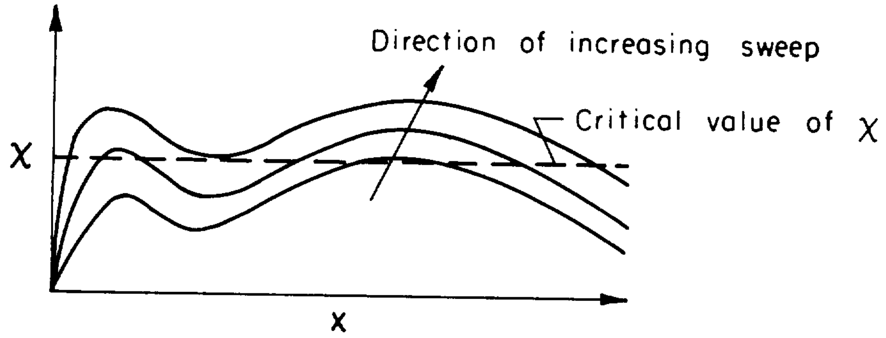

Sketch (c)

We will now examine the experimental evidence available, to see whether the effects of shock strength on transition and the changes in stability mechanism, as presented here, are consistent with available data.

Experimental evidence.- Shown in figure 7 are some available experimental results (refs. 15 and 16) for Mach numbers 3.0 and 4.0. Included in these results are transition results for both blunt flat plates (i.e., zero spanwise pressure gradient for regions farther than 20 to 30 leading-edge diameters downstream of the leading edge) and for contoured airfoils (i.e., strong spanwise pressure gradients). Also shown are the theoretical curves for the effect of shock strength on length of laminar flow. The value of ω, the exponent in the viscosity relationship used in the shock strength equation, was chosen to correspond to the average temperature of the experimental tests of references 15 and 16.

Comparison of the theoretical shock strength predictions with the results of references 15 and 16 for blunt swept flat plates at Mach numbers 2.0, 2.5, 3.0, and 4.0 has been made in references 8 and 16; therefore, it will suffice here to say that, in general, these results agree with the theoretical predictions, provided the leading-edge diameter is large enough to give a fully effective high-entropy layer, but not so large to cause crossflow instability. The models with leading-edge diameters between 0.002 and 0.005 inch appear to be near this proper leading-edge size. The model with the sharper leading edge had insufficient bluntness and the changes in the length of laminar flow with sweep were smaller than would be predicted by theory.

For the case of strong spanwise pressure gradients, transition is usually controlled by crossflow instability. The results of reference 15 (for an NACA 65A004 airfoil at a Mach number of 4.04) as well as the results of reference 16 (for the bluntest flat plate) are examples of transition which is probably controlled by crossflow. The results for the airfoil have been normalized by the length of laminar flow for a sweep angle of 12.5° since no results were available at a sweep angle of 0°. These data probably would be somewhat lower if normalized by the length at a sweep angle of 0°; however, the relative changes with sweep would be the same. It was pointed out in the discussion that effects of changes in local Reynolds number, due to shock strength, on the relative length of laminar flow, would be less for transition controlled by crossflow than for that caused by Tollmien-Schlichting instability. This is not borne out by the results shown in figure 7. Here the measured relative change in length of laminar flow, due to sweeping either the contoured airfoil or the bluntest flat plate from 45° to 60°, is approximately the same as predicted by the shock-loss method with only Tollmien-Schlichting instability considered. This might be explained by the fact that the crossflow velocity ratio is a function of distance downstream of the leading edge, thereby resulting in larger changes in the length of laminar flow with sweep than could be explained by only Reynolds number changes.

Although the data points are not close enough together to allow for an accurate determination of the sweep angle at which the mechanism controlling transition changes (if it changes at all), there is a larger reduction in the length of laminar flow at sweep angles less than 30°

than can be explained by shock-loss considerations for both the contoured airfoil at Mach number 4.04 and the flat plate with the bluntest leading edge at Mach numbers 3.0 and 4.0. These changes, however, do not appear to be discontinuous as suggested in sketch (b).

SUMMARY OF RESULTS

In the preceding discussion the effects of crossflow and shock strength on boundary-layer transition on swept wings, at supersonic speeds, were analyzed. Following are some of the important points resulting from this analysis.

1. The crossflow stability criterion of Owen and Randall was found to apply apparently without change on cylindrical leading edges for Mach numbers from subsonic to 7. A simplified method of calculating the crossflow Reynolds number on circular leading edges was developed and applied to obtain the above result. The amount of crossflow needed to induce crossflow instability downstream of the leading edge was found to be very small - on the order of 1 to 2 percent of free-stream velocity for the conditions considered.

2. The theory based on the shock-strength considerations appears to predict the changes in length of laminar flow due to sweep for blunted flat plates, if the leading edge is blunt enough to provide a sufficiently thick high entropy layer but not so blunt as to result in change of the mechanism controlling transition. For the case of these flat plates with blunter leading edges and also for wings with large spanwise pressure gradients, the theory underpredicts the changes in length of laminar flow due to sweep.

Ames Research Center
National Aeronautics and Space Administration
Moffett Field, Calif., July 20, 1961

APPENDIX A

THE CALCULATION OF THE CROSSFLOW REYNOLDS NUMBER FOR A SWEPT SEMICIRCULAR LEADING EDGE

The crossflow Reynolds number, as defined by equation (1) of the text, may be rewritten as

$$\chi = \frac{\rho_e U_e}{\mu_e} \frac{w_{max}}{U_e} \delta \tag{A1}$$

Now let

$$\frac{\rho_e U_e}{\mu_e} = \frac{R_e}{x}$$

and

$$\frac{w_{max}}{U_e} = \beta_{max}$$

Then equation (A1) may be written

$$\chi = \frac{R_e}{x} \beta_{max} \delta \tag{A2}$$

The crossflow velocity ratio, β_{max}, may be calculated by the method described in appendix B for swept semicircular leading edges.

The value of the local unit Reynolds number may be related to that of the free stream. This is done in appendix C and may be expressed

$$\frac{R_e}{x} = \frac{R_\infty}{x} H \tag{A3}$$

where H is defined by equation (4) of appendix C. The value of the local static pressure and local Mach number can be obtained, with satisfactory accuracy for the front part of a cylinder, from the modified Newtonian pressure distribution given in reference 9:

$$\frac{p_e}{p_s} = \left(1 - \frac{p_\infty}{p_s}\right) \cos^2\theta + \frac{p_\infty}{p_s} \tag{A4}$$

where p_s is the static pressure on the stagnation line.

The only remaining quantity to be determined is the boundary-layer thickness, δ. For the case of a circular leading edge, δ is assumed to be constant and equal to the stagnation-line value. This approximation holds for a large portion of a blunt leading edge normal to the free stream and is assumed to hold for swept leading edges. The value at the stagnation line is given in reference 6 as

$$\delta = \frac{B(T_W/T_O)^{-1}}{\sqrt{(U_\infty \rho_W/\mu_W D)[(D/U_\infty)(dU_e/dx)]}} \tag{A5}$$

where B, the boundary-layer thickness parameter is the integral through the boundary layer of a function of enthalpy which appears in equation 56 of reference 6. The velocity gradient parameter

$$G \equiv \frac{D}{U_\infty}\frac{dU_e}{dx} \tag{A6}$$

is determined by equations 62 and 63 of reference 6. Values of B and G are plotted as functions of the flow parameters in reference 6. The equation of state for a perfect gas and the viscosity relationship

$$\mu = \mu_\infty \left(\frac{T}{T_\infty}\right)^{\omega} \tag{A7}$$

may be used to write the boundary-layer thickness as:

$$\delta = \frac{BD^{\frac{1}{2}}(T_W/T_O)^{\frac{\omega-1}{2}}(T_O/T_\infty)^{\frac{\omega+1}{2}}}{(R_\infty/x)^{\frac{1}{2}}G^{\frac{1}{2}}(p_s/p_\infty)^{\frac{1}{2}}} \tag{A8}$$

We may now write the expression for the crossflow Reynolds number on a swept circular leading edge:

$$\frac{\chi}{\sqrt{R_\infty(D/x)}} = \frac{(T_O/T_\infty)^{\frac{\omega+1}{2}}(T_W/T_O)^{\frac{\omega-1}{2}}}{\sqrt{G(p_s/p_\infty)}}\,HB\beta_{max} \tag{A9}$$

where the quantities H and β_{max} are functions of free-stream Mach number, sweep angle, ratio of wall-to-free-stream total temperature, and local flow properties. All other quantities are functions of all the things listed above except the local flow properties.

APPENDIX B

THE CALCULATION OF THE CROSSFLOW VELOCITY RATIO β

In finding the value of the crossflow velocity ratio, $\beta = w/U_e$, the stagnation-line solutions (ref. 6) for the velocity profile, parallel and normal to the leading edge, are used over the entire leading edge. The results are shifted to a different set of coordinates, along and normal to the local boundary-layer-edge streamline as shown below

A
4
6
1

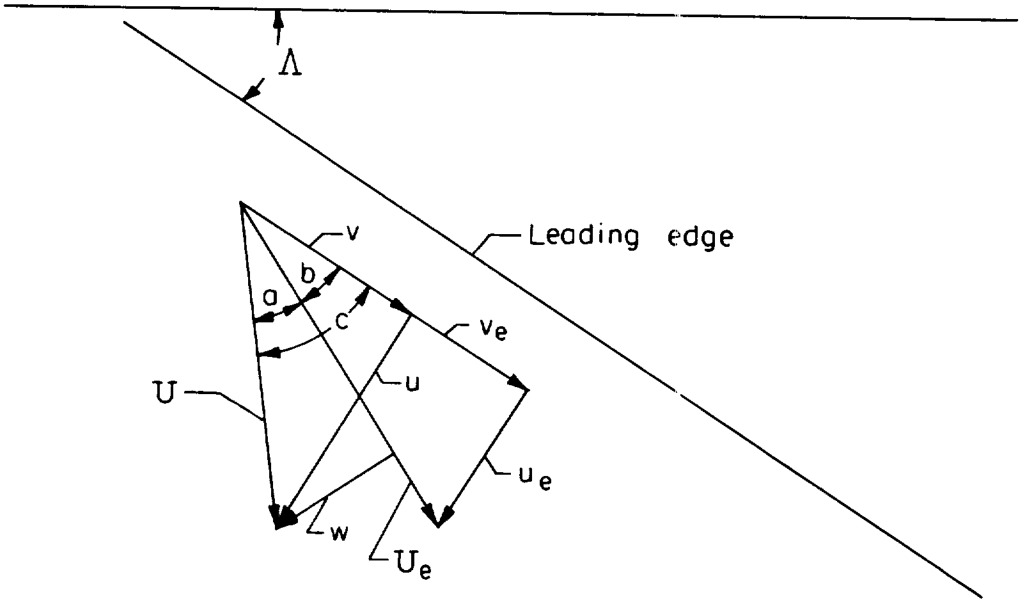

where

$$U = (u^2 + v^2)^{1/2} \tag{B1}$$

and

$$u = f'U_e \sin b \qquad f' = u/u_e$$

$$v = gU_e \cos b \qquad g = v/v_e$$

Therefore,

$$U/U_e = \sin b \, (f'^2 + g^2\cot^2 b)^{1/2} \tag{B2}$$

$$w = U \sin a$$

$$w/U_e = \sin a \sin b \, (f'^2 + g^2\cot^2 b)^{1/2} \tag{B3}$$

where f' and g are obtained from reference 6 and are functions of T_w/T_o, M_∞, Λ, Prandtl number, and the distance normal to surface. The angle b is a function of the potential flow and may be determined from the pressure distribution. The velocity component parallel to the shock wave, which is unaltered as it passes through the shock, is also assumed to remain the same around the leading edge. This is true for a wing extending to infinity in both directions. The total velocity may be found from the pressure distribution given by equation (A4). This is done by changing the pressure ratio from a ratio of static pressures, p_e/p_s, to a ratio of static pressure to total pressure downstream of the shock, p_e/p_t. From this ratio the resultant Mach number, and thus the resultant velocity, may be obtained. The ratio of velocity parallel to the shock wave to the total velocity is the cosine of angle b. Angle a is a function of both angle b and the boundary-layer flow angle c. The relationship is as follows:

$$\tan c = \frac{f'}{g} \tan b \tag{B4}$$

and

$$c = a + b$$

therefore

$$\tan a = \frac{(\tan b)[(f'/g) - 1]}{1 + (f'/g) \tan^2 b} \tag{B5}$$

The crossflow velocity profile may be obtained from equations (B3) and (B5). Figure 8 shows some typical crossflow profiles for the case of a sweep angle of 75° temperature ratio equal to zero, and a local stream angle of 10°. Curves are presented for various Mach numbers.

APPENDIX C

THE EFFECT OF SHOCK STRENGTH ON LENGTH OF LAMINAR RUN

The expression for the Reynolds number

$$R = \frac{\rho U x}{\mu} \tag{C1}$$

may be rewritten in terms of

$$U = M\sqrt{\gamma ST} \tag{C2a}$$

$$\rho = p/ST \tag{C2b}$$

$$\mu = \mu_\infty (T/T_\infty)^\omega \tag{C2c}$$

to give

$$R = \frac{pM}{\mu_\infty}\left(\frac{T_\infty}{T}\right)^\omega \sqrt{\frac{\gamma}{ST}}\; x \tag{C3}$$

where S is the gas constant. If we now take the ratio of local to free-stream unit Reynolds number, we obtain:

$$\frac{R_e/x}{R_\infty/x} = \frac{p_e}{p_\infty}\frac{M_e}{M_\infty}\left(\frac{T_\infty}{T_e}\right)^{\frac{2\omega+1}{2}} = H \tag{C4}$$

Now taking the value of equation (C4) for a given sweep angle and dividing by the value of equation (C4) at zero sweep, we get

$$\frac{\left(\dfrac{R_e/x}{R_\infty/x}\right)_\Lambda}{\left(\dfrac{R_e/x}{R_\infty/x}\right)_{\Lambda=0}} = \frac{\left(\dfrac{R_e}{x}\right)_\Lambda}{\left(\dfrac{R_e}{x}\right)_{\Lambda=0}} = \frac{(p_e M_e)_\Lambda}{(p_e M_e)_{\Lambda=0}}\left[\frac{(T_e)_{\Lambda=0}}{(T_e)_\Lambda}\right]^{\frac{2\omega+1}{2}} \tag{C5}$$

Assuming that the transition Reynolds number R_e is a constant based on x_l to transition, then

$$\frac{(R_e)_\Lambda}{(R_e)_{\Lambda=0}} = 1 \tag{C6}$$

and therefore

$$\frac{(x_l)_\Lambda}{(x_l)_{\Lambda=0}} = \frac{(R_e/x)_{\Lambda=0}}{(R_e/x)_\Lambda} \tag{C7}$$

Now from equations (C5) and (C7) the ratio of the length of laminar flow for a given sweep angle to that for zero sweep is

$$\frac{(x_l)_\Lambda}{(x_l)_{\Lambda=0}} = \frac{(p_eM_e)_{\Lambda=0}}{(p_eM_e)_\Lambda}\left[\frac{1+\frac{\gamma-1}{2}(M_e)^2_{\Lambda=0}}{1+\frac{\gamma-1}{2}(M_e)^2_\Lambda}\right]^{\frac{2\omega+1}{2}} \tag{C8}$$

The values of static pressure and Mach numbers are functions of shock strength and geometry of the body. The shock strength is determined by the normal Mach number.

Equation (C8) may be simplified by the following assumptions:

(1) The flat plate, is sufficiently blunt that the length of laminar flow is maximum.

(2) The shock wave lies parallel to the leading edge (up to the point where normal Mach number equals 1) when the wing is swept.

(3) The region considered is sufficiently far behind the leading edge (20 to 30 leading-edge thicknesses) that the static pressure has reached the free-stream value.

Using these assumptions, equation (C9) reduces to:

$$\frac{(x_l)_\Lambda}{(x_l)_{\Lambda=0}} = \frac{(M_e)_{\Lambda=0}}{(M_e)_\Lambda}\left[\frac{1+\frac{\gamma-1}{2}(M_e)^2_{\Lambda=0}}{1+\frac{\gamma-1}{2}(M_e)^2_\Lambda}\right]^{\frac{2\omega+1}{2}} \tag{C9}$$

where the Mach numbers may be determined from reference 17 by evaluating the following functions

$$M_e = E\left(\frac{p_e}{p_{t_e}}\right) \tag{C10}$$

$$\frac{p_e}{p_{t_e}} = \frac{p_\infty}{p_{t_\infty}}\,\frac{p_{t_\infty}}{p_{t_e}} \tag{C11a}$$

$$\frac{p_\infty}{p_{t_\infty}} = F(M_\infty) \tag{C11b}$$

$$\frac{p_{t_\infty}}{p_{t_e}} = J(M_\infty \cos \Lambda) \tag{C11c}$$

The ideas introduced in equation (C6) and following have significance only with respect to Tollmien-Schlichting type instability.

A
4
6
1

REFERENCES

1. Owen, P. R., and Randall, D. G.: Boundary Layer Transition on a Swept back Wing. R.A.E. TM Aero 277, May 1952.

2. Moeckel, W. E.: Some Effects of Bluntness on Boundary-Layer Transition and Heat Transfer at Supersonic Speeds. NACA Rep. 1312, 1957. (Supersedes NACA TN 3653)

3. Gregory, N., Stuart, J. T., and Walker, W. S.: On the Stability of Three-Dimensional Boundary Layers with Application to Flow Due to a Rotating Disk. Phil. Trans. Royal Society (London), series A, vol. 248, no. 943, July 14, 1955, pp. 155-199.

4. Boltz, Fredrick W., Kenyon, George C., and Allen, Clyde Q.: Effects of Sweep Angle on the Boundary-Layer Stability Characteristics of an Untapered Wing at Low Speeds. NASA TN D-338, 1960.

5. Scott-Wilson, J. B., and Capps, D. S.: Wind Tunnel Observation of Boundary Layer Transition on Two Sweptback Wings at a Mach Number of 1.61. R.A.E. TN Aero 2347, Dec. 1954.

6. Reshotko, Eli, and Beckwith, Ivan E.: Compressible Laminar Boundary Layer Over a Yawed Infinite Cylinder with Heat Transfer and Arbitrary Prandtl Number. NACA Rep. 1379, 1958. (Supersedes NACA TN 3986)

7. Seiff, Alvin, Sommer, Simon C., and Canning, Thomas N.: Some Experiments at High Supersonic Speeds on the Aerodynamic and Boundary-Layer Transition Characteristics of High-Drag Bodies of Revolution. NACA RM A56I05, 1957.

8. Beckwith, Ivan E., and Gallagher, James J.: Experimental Investigation of the Effect of Boundary-Layer Transition on the Average Heat Transfer to a Yawed Cylinder in Supersonic Flow. NACA RM L56E09, 1956.

9. Beckwith, Ivan E., and Gallagher, James J.: Local Heat Transfer and Recovery Temperature on a Yawed Cylinder at a Mach Number of 4.15 and High Reynolds Number. NACA MEMO 2-27-59L, 1959.

10. Feller, William V.: Investigation of Equilibrium Temperatures and Average Laminar Heat-Transfer Coefficients for the Front Half of Swept Circular Cylinders at a Mach number of 6.9. NACA RM L55F08a, 1955.

11. Goodwin, Glen, and Creager, Marcus O.: Investigation of Local Heat Transfer and Pressure Drag Characteristics of a Yawed Circular Cylinder at Supersonic Speeds. NACA RM A55H31, 1955.

12. Van Driest, E. R.: Investigation of Laminar Boundary Layer in Compressible Fluids Using the Crocco Method. NACA TN 2597, 1952.

13. Chapman, Gary T.: Transition of the Laminar Boundary Layer on a Delta Wing With 74° Sweep in Free Flight at Mach Numbers From 2.8 to 5.3. NASA TN D-1066, 1961.

14. Brinich, Paul F.: Effect of Leading-Edge Geometry on Boundary-Layer Transition at Mach Number 3.1. NACA TN 3659, 1956.

15. Dunning, Robert W., and Ulmann, Edward F.: Effect of Sweep and Angle of Attack on Boundary-Layer Transition on Wings at Mach Number 4.04. NACA TN 3473, 1955.

16. Jillie, Don W., and Hopkins, Edward J.: Effects of Mach Number, Leading-Edge Bluntness, and Sweep on Boundary-Layer Transition on a Flat Plate. NASA TN D-1071, 1961.

17. Ames Research Staff: Equations, Tables, and Charts for Compressible Flow. NACA Rep. 1135, 1953.

TABLE I.- CRITICAL CROSSFLOW REYNOLDS NUMBERS

Λ, deg	M_∞	T_w/T_o	$\frac{R_\infty D}{x} \times 10^{-6}$	X_{max}	Reference	State of boundary layer	Heat transfer measurement
10	4.15	0.80	1.39	177	9	Laminar	Local
			2.33	229		Turbulent	
↓			3.77	291			
20			1.31	209			
↓			1.78	243			
			3.12	322	↓		↓
30			1.3	260	8		Average
	↓	↓	.5	161	8	↓	Average
	3.90	1.1	.007	23	11	Laminar	Local
↓	6.90	0.5-0.8	.13	60	10	Laminar	Average
45	4.15	0.80	1.3	375	8	Turbulent	
	4.15	0.80	.5	232	8	Turbulent	↓
	3.90	1.1	.007	33	11	Laminar	Local
↓	6.90	0.5-0.8	.13	84	10	Laminar	Average
60	4.15	0.8	1.3	505	8	Turbulent	
	4.15	0.8	.5	313	8	Turbulent	
↓	6.9	0.5-0.8	.13	141	10	Transitional	
75	6.9	0.5-0.8	.13	194	10	Turbulent	↓

A
4
6
1

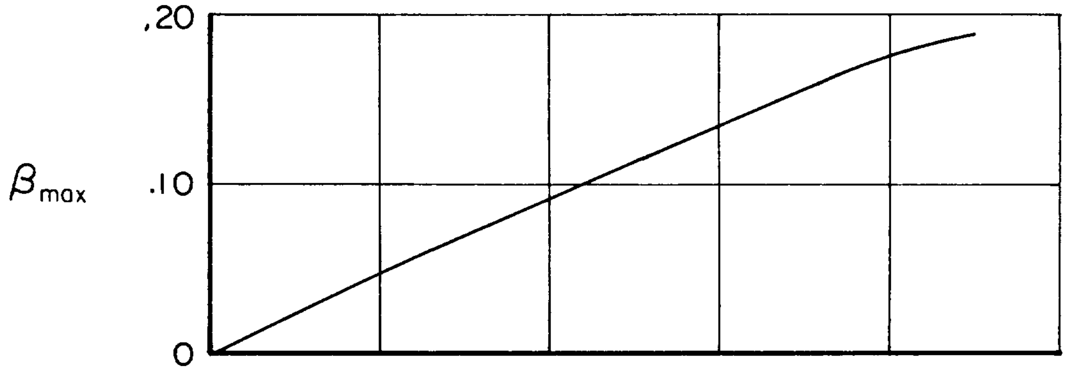

(a) Crossflow velocity ratio.

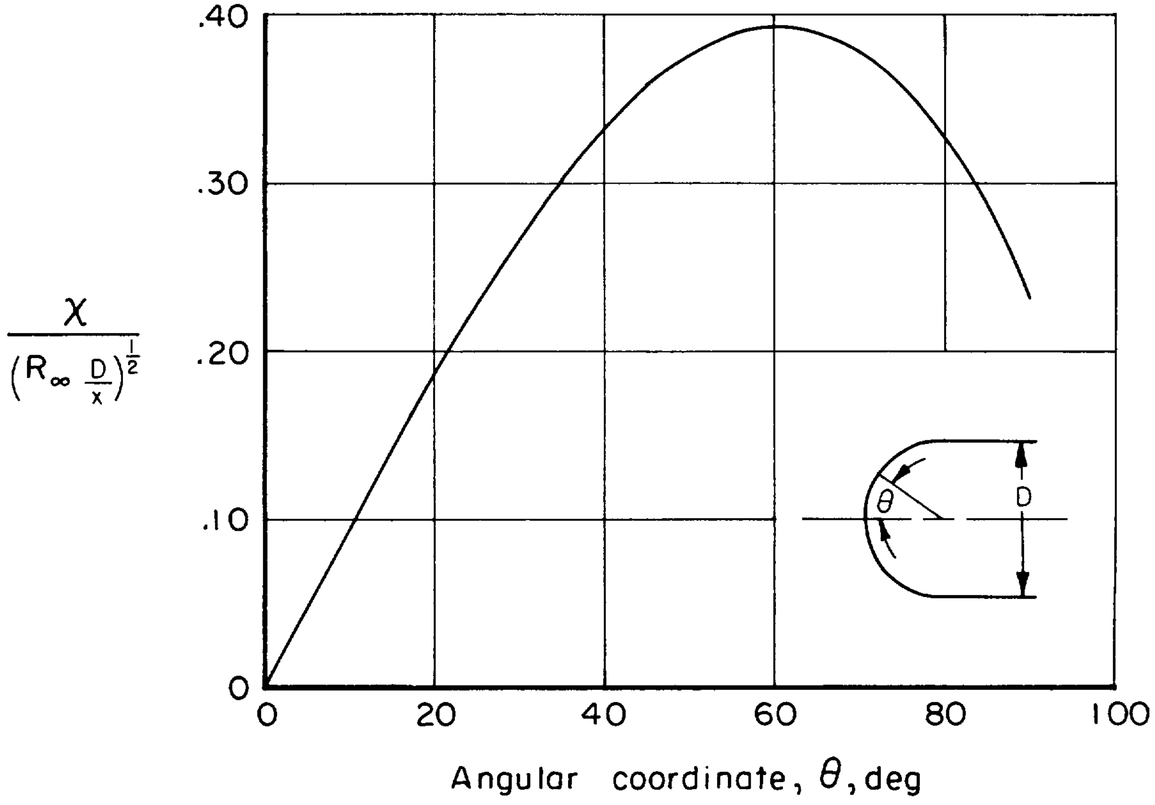

(b) Normalized crossflow Reynolds number.

Figure 1.- Flow parameters around a leading edge with 60° sweep; $M_\infty = 7.0$, $T_w/T_o = 0.6$.

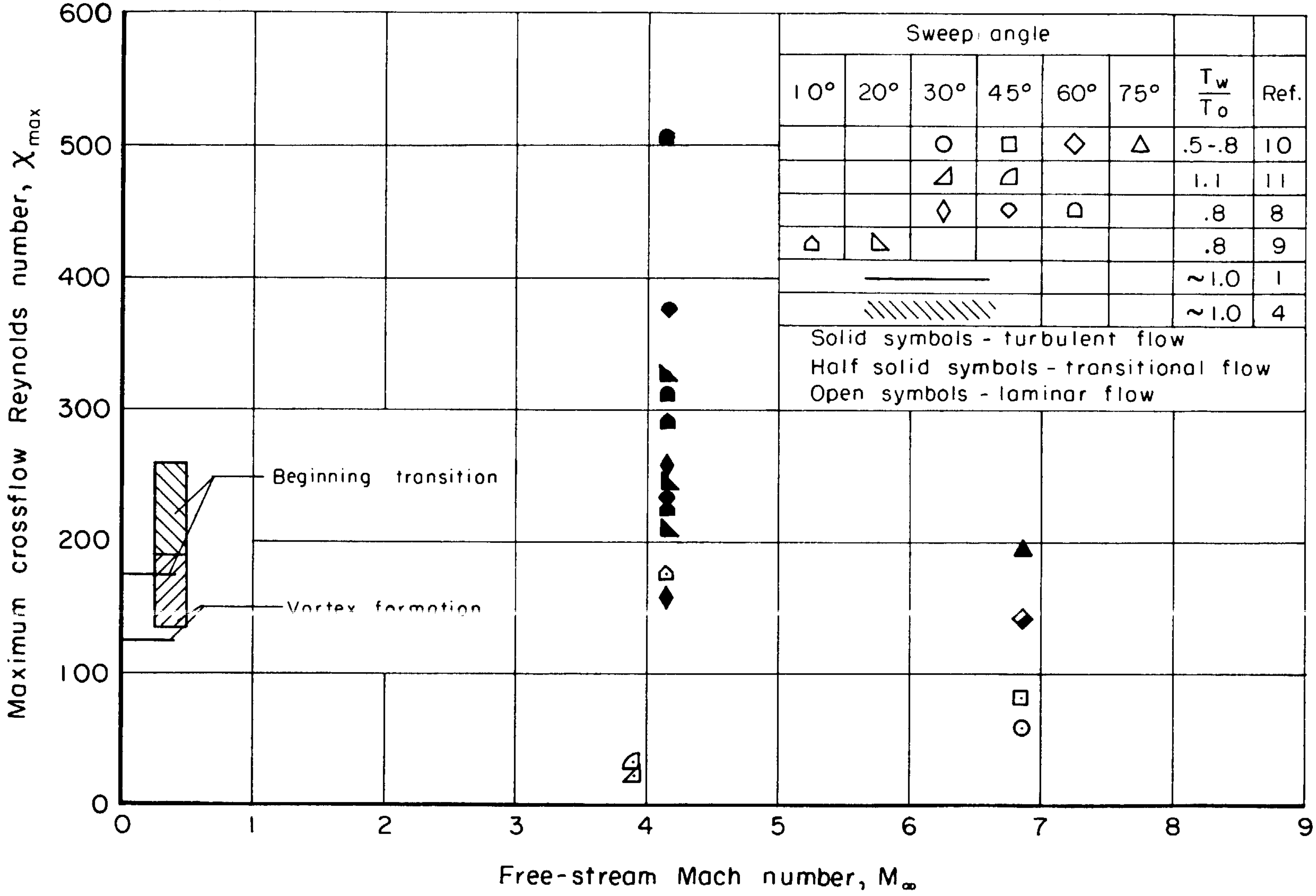

Figure 2.- Critical crossflow Reynolds number.

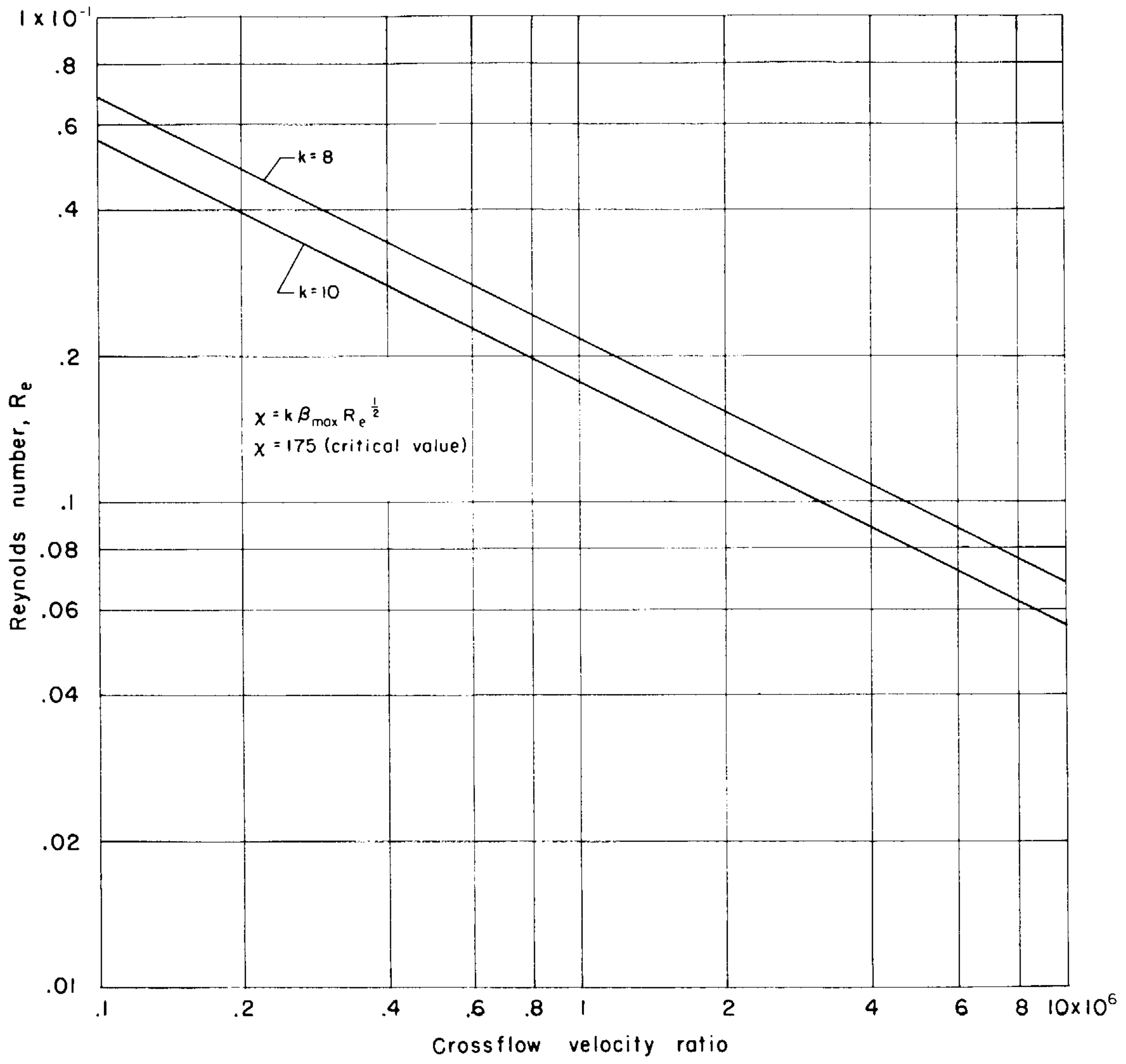

Figure 3.- Critical crossflow over surfaces where the boundary-layer growth can be approximated by two-dimensional theory.

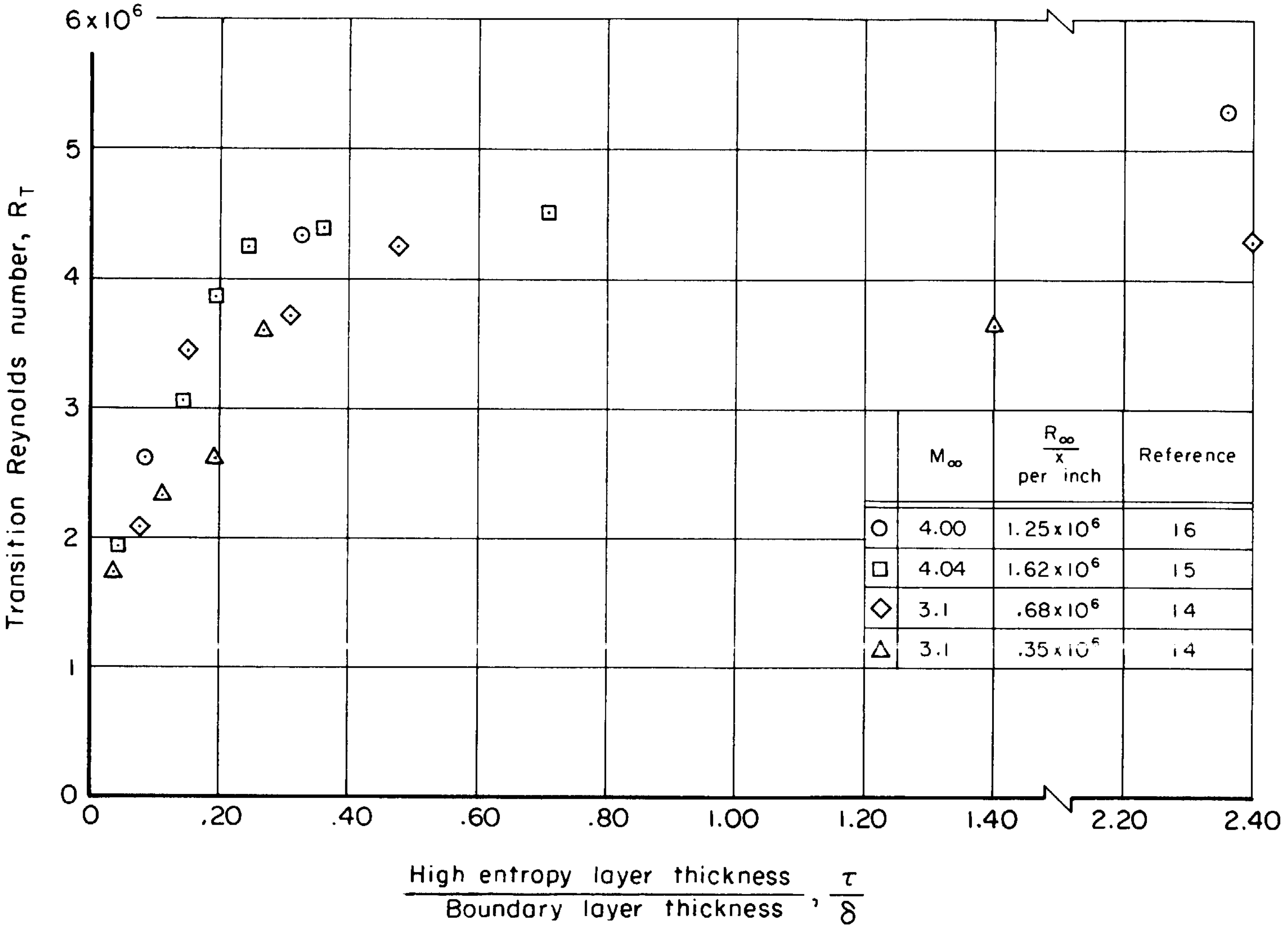

Figure 4.- Effects of the ratio of high entropy layer to boundary-layer thickness on transition Reynolds number.

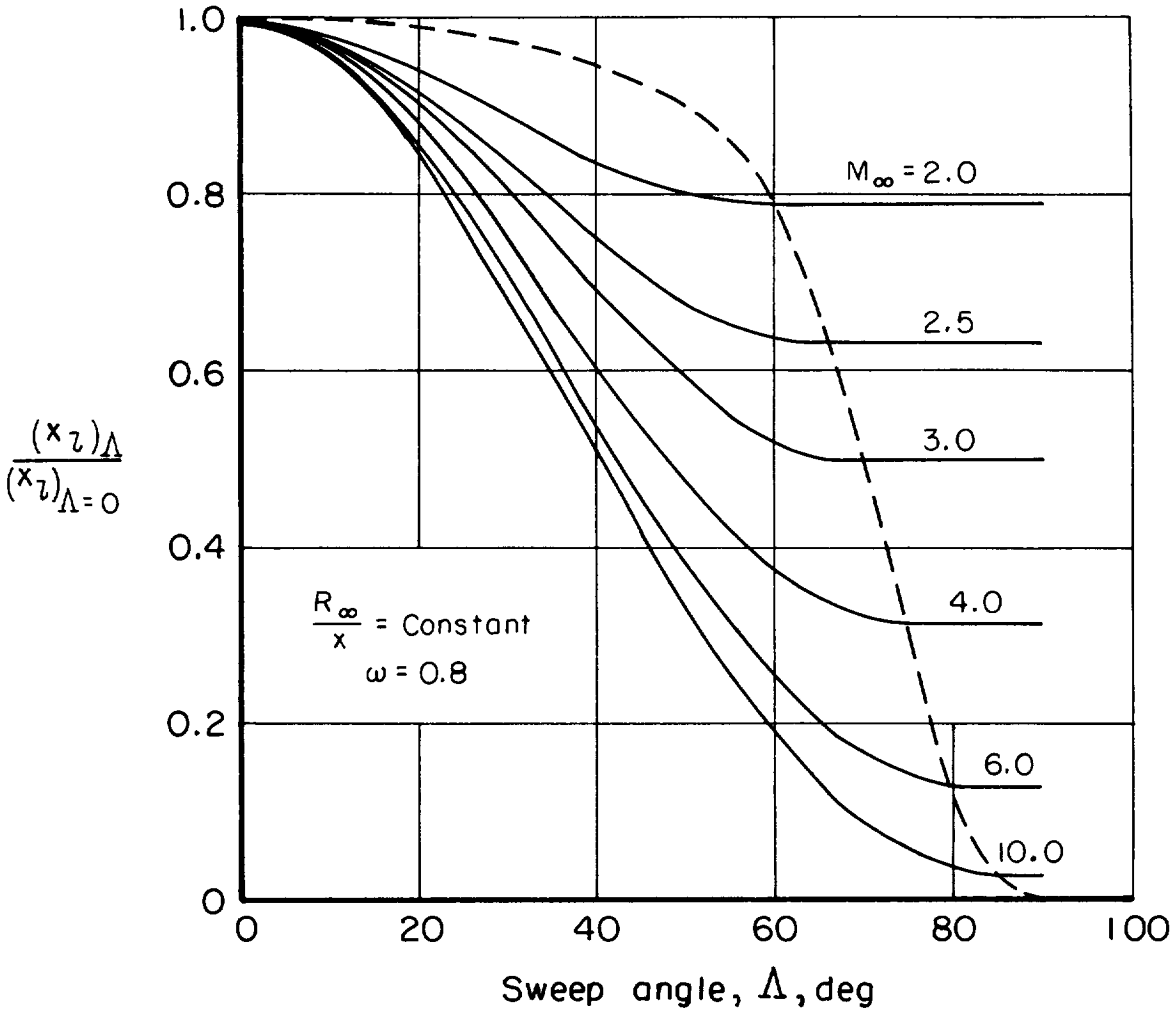

Figure 5.- Effect of shock strength on normalized length of laminar flow.

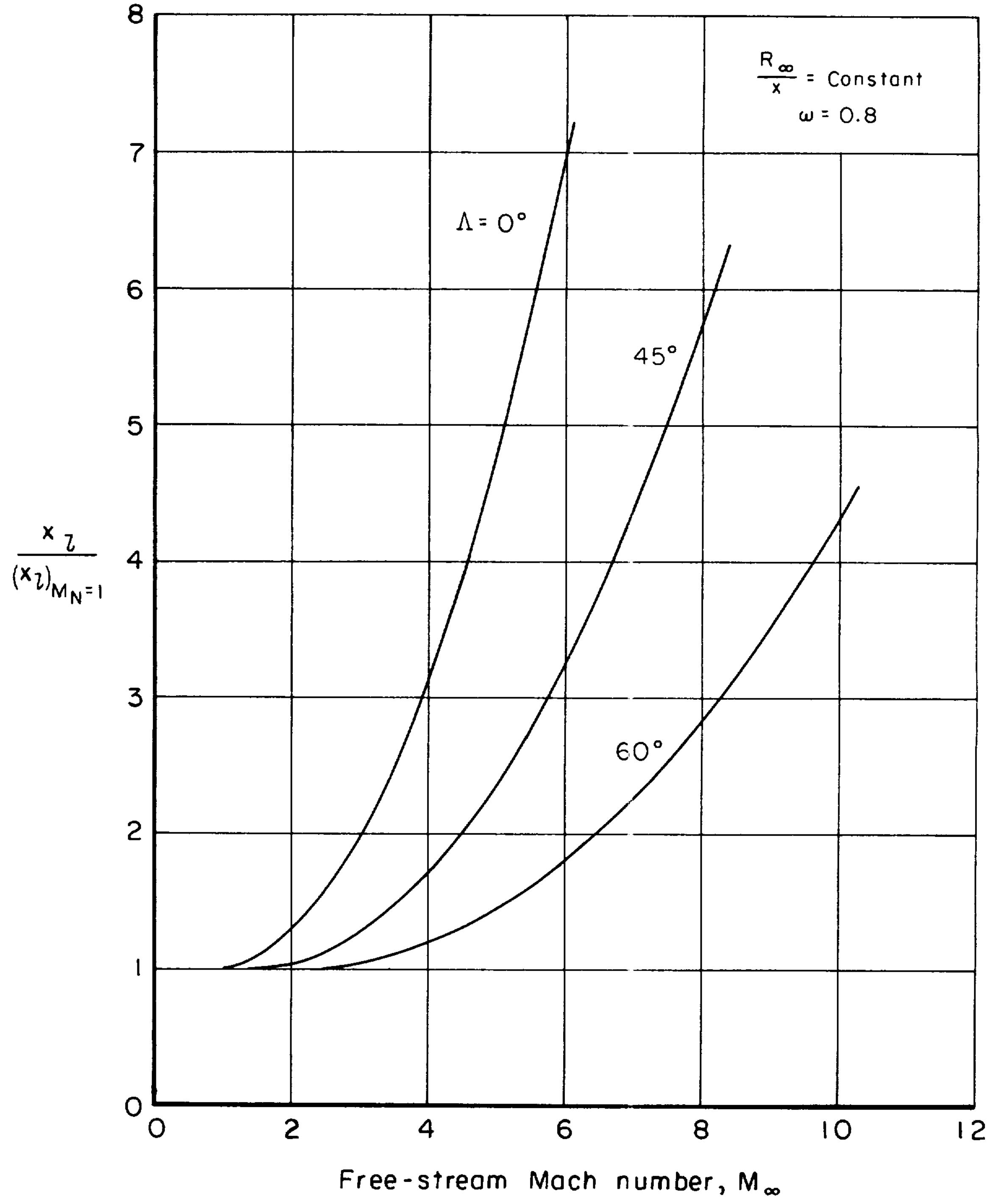

Figure 6.- Effect of shock strength on normalized length of laminar flow at constant sweep angle.

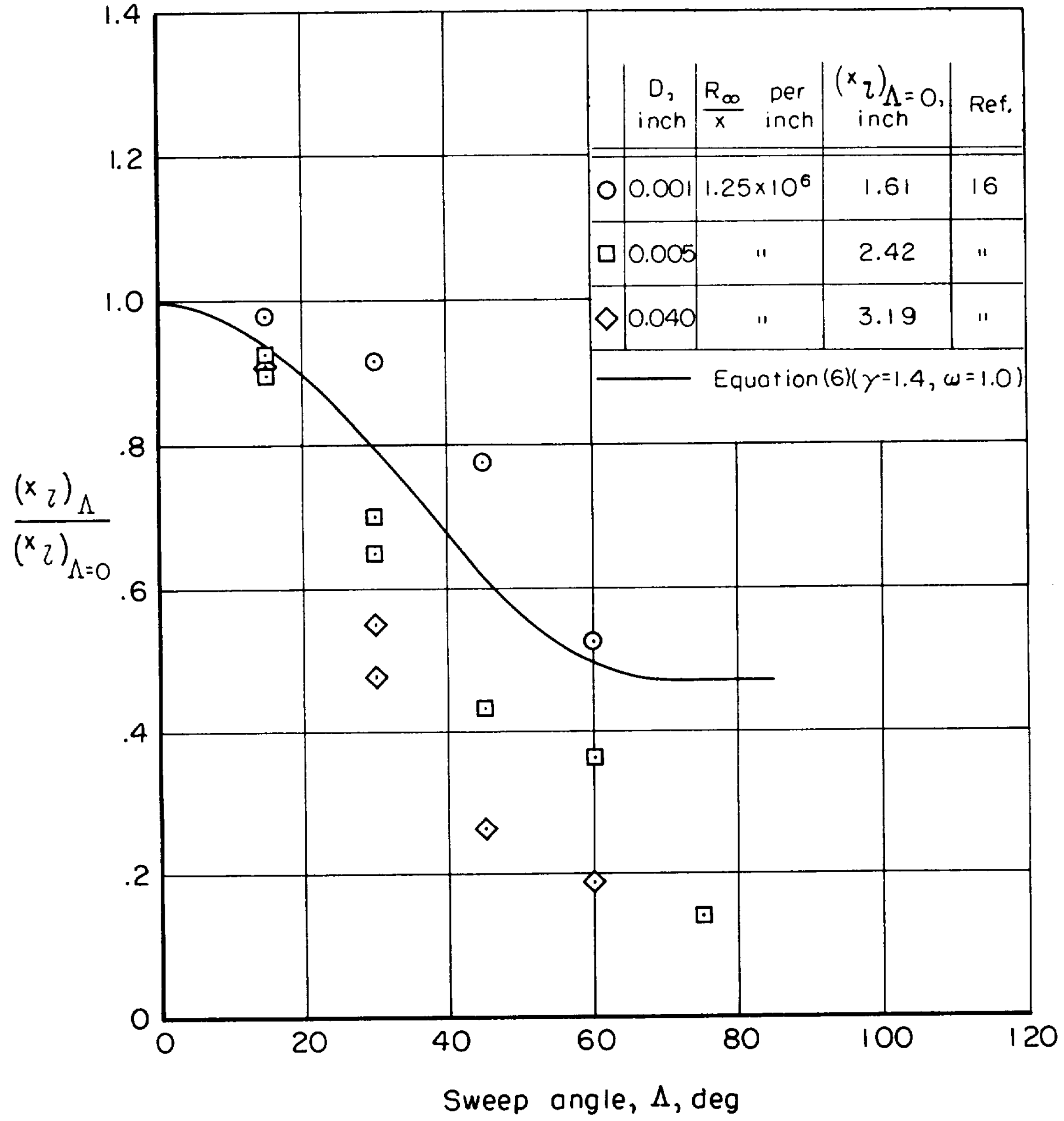

(a) $M_\infty = 3.0$

Figure 7.- The effects of sweep on the normalized length of laminar flow.

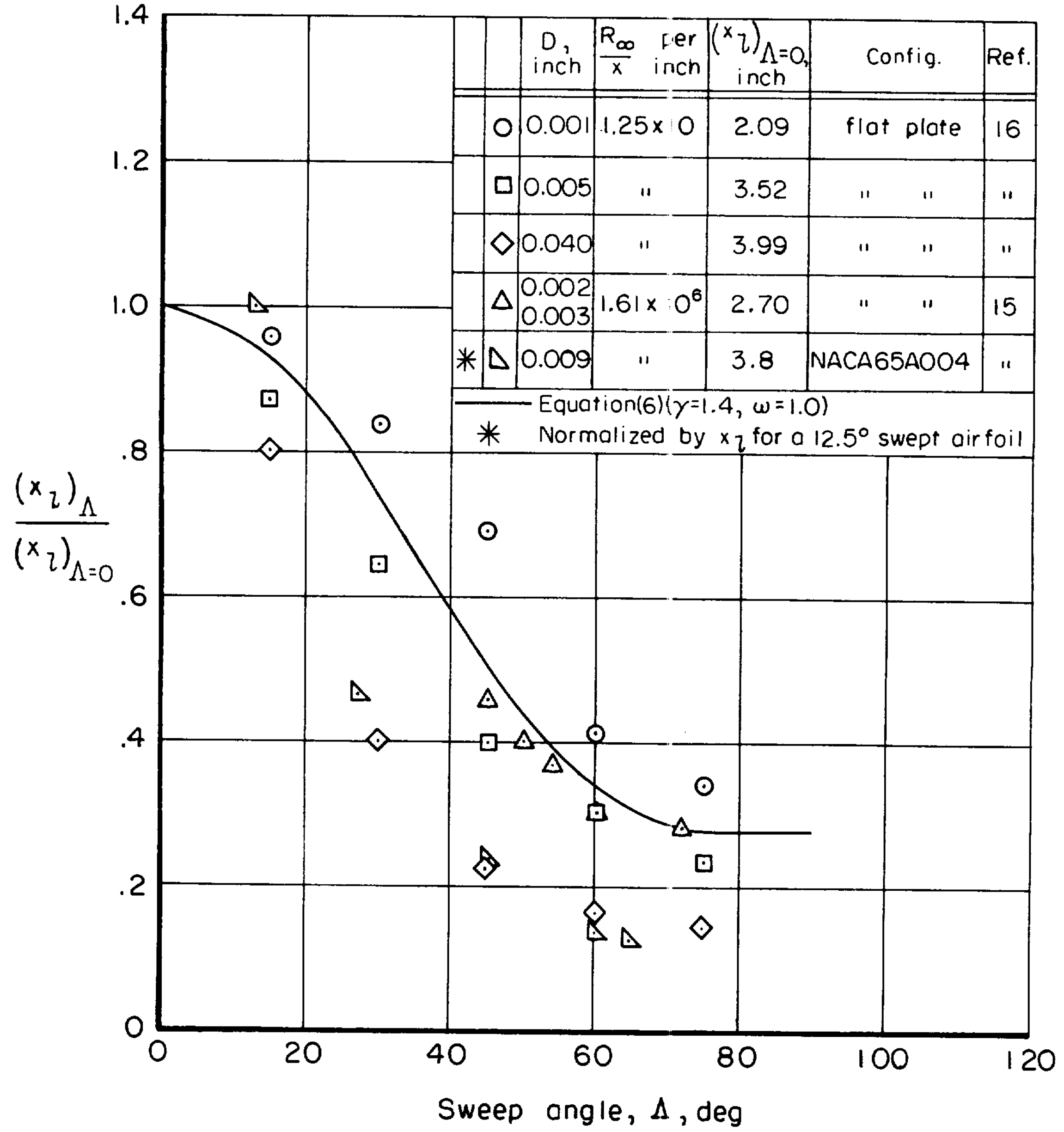

(b) $M_\infty = 4.0$

Figure 7.- Concluded.

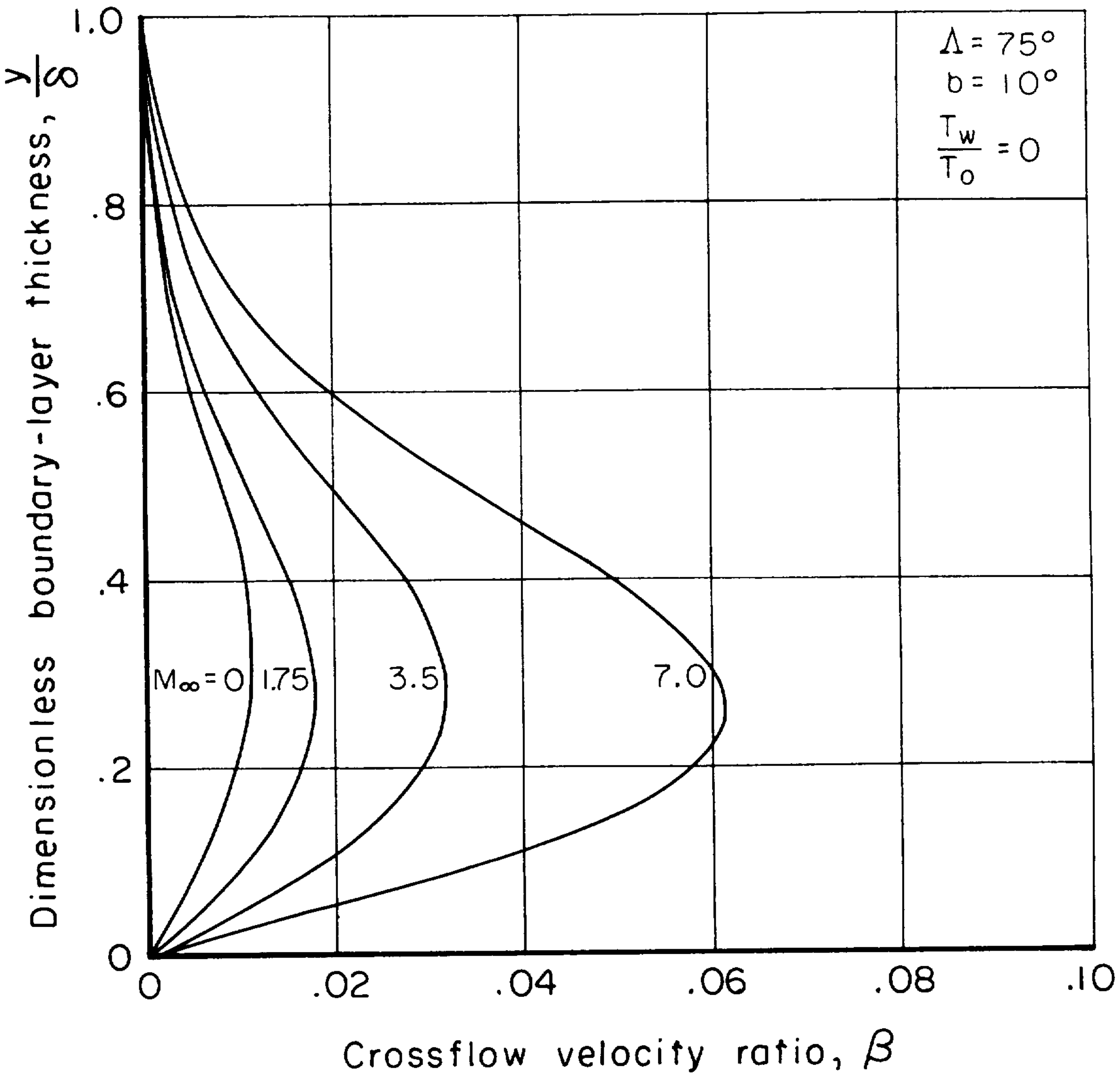

Figure 8.- Boundary-layer crossflow velocity profile.

NASA TN D-1075
National Aeronautics and Space Administration.
SOME EFFECTS OF LEADING-EDGE SWEEP ON BOUNDARY-LAYER TRANSITION AT SUPERSONIC SPEEDS. Gary T. Chapman. September 1961. 33p. OTS price, $1.00. (NASA TECHNICAL NOTE D-1075)

The effects of cross flow and shock strength on transition of the laminar boundary layer behind a swept leading edge are discussed. The critical cross-flow Reynolds number evaluated for available supersonic data indicates a wide range of applicability of the critical values given by Owen and Randall. The known effects of shock strength on transition controlled by Tollmien-Schlichting instability are also considered for swept wings.

Copies obtainable from **NASA**, Washington

I. Chapman, Gary T.
II. NASA TN D-1075

(Initial NASA distribution:
1, Aerodynamics, aircraft;
2, Aerodynamics, missiles and space vehicles;
20, Fluid mechanics.)

NASA

NASA TN D-1075
National Aeronautics and Space Administration.
SOME EFFECTS OF LEADING-EDGE SWEEP ON BOUNDARY-LAYER TRANSITION AT SUPERSONIC SPEEDS. Gary T. Chapman. September 1961. 33p. OTS price, $1.00. (NASA TECHNICAL NOTE D-1075)

The effects of cross flow and shock strength on transition of the laminar boundary layer behind a swept leading edge are discussed. The critical cross-flow Reynolds number evaluated for available supersonic data indicates a wide range of applicability of the critical values given by Owen and Randall. The known effects of shock strength on transition controlled by Tollmien-Schlichting instability are also considered for swept wings.

Copies obtainable from **NASA**, Washington

I. Chapman, Gary T.
II. NASA TN D-1075

(Initial NASA distribution:
1, Aerodynamics, aircraft;
2, Aerodynamics, missiles and space vehicles;
20, Fluid mechanics.)

NASA

NASA TN D-1075
National Aeronautics and Space Administration.
SOME EFFECTS OF LEADING-EDGE SWEEP ON BOUNDARY-LAYER TRANSITION AT SUPERSONIC SPEEDS. Gary T. Chapman. September 1961. 33p. OTS price, $1.00. (NASA TECHNICAL NOTE D-1075)

The effects of cross flow and shock strength on transition of the laminar boundary layer behind a swept leading edge are discussed. The critical cross-flow Reynolds number evaluated for available supersonic data indicates a wide range of applicability of the critical values given by Owen and Randall. The known effects of shock strength on transition controlled by Tollmien-Schlichting instability are also considered for swept wings.

Copies obtainable from **NASA**, Washington

I. Chapman, Gary T.
II. NASA TN D-1075

(Initial NASA distribution:
1, Aerodynamics, aircraft;
2, Aerodynamics, missiles and space vehicles;
20, Fluid mechanics.)

NASA

NASA TN D-1075
National Aeronautics and Space Administration.
SOME EFFECTS OF LEADING-EDGE SWEEP ON BOUNDARY-LAYER TRANSITION AT SUPERSONIC SPEEDS. Gary T. Chapman. September 1961. 33p. OTS price, $1.00. (NASA TECHNICAL NOTE D-1075)

The effects of cross flow and shock strength on transition of the laminar boundary layer behind a swept leading edge are discussed. The critical cross-flow Reynolds number evaluated for available supersonic data indicates a wide range of applicability of the critical values given by Owen and Randall. The known effects of shock strength on transition controlled by Tollmien-Schlichting instability are also considered for swept wings.

Copies obtainable from **NASA**, Washington

I. Chapman, Gary T.
II. NASA TN D-1075

(Initial NASA distribution:
1, Aerodynamics, aircraft;
2, Aerodynamics, missiles and space vehicles;
20, Fluid mechanics.)

NASA